Desalination and Water Treatment
www.deswater.com

doi: 10.5004/dwt.2023.29139

281 (2023) 204–216
January

Optimization of chemical oxygen demand removal from petroleum refinery wastewater by electrocoagulation using tubular electrochemical reactor with a novel design

Ghazi Faisal Naser[a,*], Thamer J. Mohammed[b], Ali H. Abbar[c]

[a]*Chemical Engineering Department, College of Engineering, Al-Muthanna University, Iraq, Tel.: +9647826567773; email: ghazi_faisal@mu.edu.iq*
[b]*Chemical Engineering Department, University of Technology, Baghdad, Iraq, Tel.: +9647711300372; email: thamer.j.mohammed@uotechnology.edu.iq*
[c]*Department of Biochemical Engineering, Al-Khwarizmi College of Engineering, University of Baghdad, Baghdad, Iraq, Tel.: +964 7803280891; email: ali.abbar@kecbu.uobaghdad.edu.iq*

Received 28 July 2022; Accepted 21 November 2022

ABSTRACT

In this study, removal of chemical oxygen demand (COD) from petroleum refinery effluent was investigated using a new tubular electrochemical reactor (TER) design which operated at a batch recycle model. The electrochemical reactor comprises of two concentric electrodes namely spiral aluminum rode anode and hollow cylindrical stainless steel cathode. Four parameters were investigated: current density, sodium chloride concentration (NaCl), pH, and flow rate on the COD removal efficiency, and optimized using response surface methodology. Results show that current density is the most influential parameter on removal percentage where increasing current density results in increasing the removal efficiency. Another effect of lowering flow rate resulted in high removal of COD due to the increased resistance time of effluent passing on the surface of the anode with the newly adopted design. Finding of laboratory work were obtained under optimal working conditions such as current density of 26 mA/cm^2, pH of 7.9, NaCl concentration of 1.1 g/L, and flow rate of 2 L/min. These were resulting in a COD removal efficiency of 73.36% with specific energy consumption of 30.61 kWh/kg·COD. Operating cost of the present system was found to be \$2.185 m^3 which is considered low and acceptable. Experimental results prove that the new design of TER is more efficient than the traditional design that uses in electrocoagulation system to treat wastewater generated from petroleum refinery plants.

Keywords: Electrocoagulation; Tubular electrochemical reactor; Spiral anode; Chemical oxygen demand removal; Petroleum refinery wastewater

1. Introduction

In refining crude oil, petroleum refineries consume huge amounts of fresh water as a cooling agent [1,2]. Similarly, too much quantity of wastewater are generated; for a daily crude oil yield of 13 million metric tons (84 million barrels). Mustapha et al. [3] and Diya'uddeen et al. [4] reported that the amount of effluent generated by refineries during processing ranges from 0.04 to 1.66 times the amount of crude oil processed, with 5.3 million metric tons (m^3) being the global average for total effluent production. The accumulation of undesired industrial by-products dumped into the environment without treatment is dangerous [5,6]. Before releasing crude oil wastewater into the environment or reusing for irrigation, livestock, groundwater replenishment, and many other applications must be effectively

* Corresponding author.

treated [7]. Scientists and engineers have studied remediation possibilities of plants for various contaminants in polluted waterways [3,8–10]. Generally, crude oil wastewater involves organic compounds and heavy metals, thus several methods are found for treating such types of effluents and listed as chemical precipitation [11,12], coagulation/flocculation [13,14], adsorption [11,15], membranes [16,17], and biological methods [18]. In addition, these ways offer different typical benefits such as versatility, environmental compatibility and energy efficiency [19].

In comparison to traditional techniques, electrochemical coagulation is one of the electrochemical treatment methods that received remarkable attention in recent years as an efficient treating wastewater technique. Electrocoagulation is an electrochemical type commonly used to process water and wastewater because its ability to simultaneously remove a broad range of contaminants. In contrast to biological treatment methods, which require a certain condition to manufacture coagulants, the electrocoagulation method may solve this difficulty since it is environmentally friendly, safe, energy-efficient, and cost-effective [20,21]. Electrocoagulation developed from the concept of the destabilization of harmful colloidal particles by adding certain metal salts like alum ($Al_2(SO_4)_3$), iron sulfate, and iron chloride, where these colloidal particles will be surrounded by the electrical double layer squeezed by the positive charge of cations [22]. Similarly, electro-floatation is used in conjunction with electrocoagulation to remove contaminants. This process involves the emission of hydrogen gas from the cathode electrode to enhance the flocculated particle buoyancy operation at the surface of the treated wastewater [22,23]. The reactions of electrochemical techniques that occur during electrochemical oxidation are simply involved in the released ions by the oxidation of the artificial anode made from a particular metal. The decomposition of the anode in polluted water produces counter ions that neutralize the ionic presence in the contaminated water, resulting in a Van der Waals attraction force and a reduction in electrostatic inter-particle repulsion. This leads to zero net charges and the coagulation process [24]. As a result, a sludge-like layer of colloidal particles is generated in the form of flocs. In the classic chemical precipitation approach, it is easier to precipitate out these flocs since they are bigger, heavier and contain less bound water [25]. Eqs. (1) and (2) at the anode electrode, while Eq. (3) at the cathode electrode.

The reactions that take place in the EC process can be summarized as follows:

At the anode:

$$\left(\mathrm{Al}\right)_{(s)} \rightarrow \mathrm{Al}^{3+}_{(aq)} + 3e^- \tag{1}$$

$$2\mathrm{H_2O} \rightarrow \mathrm{O}_{2(g)} + 5\mathrm{H}^+ + 5e^- \tag{2}$$

At the cathode:

$$2\mathrm{H_2O} + 2e^- \rightarrow \mathrm{H_2} + 2\mathrm{OH}^- \tag{3}$$

In solution:

$$\mathrm{Al}^{3+} + 3\mathrm{OH}^- \rightarrow \mathrm{Al}\left(\mathrm{OH}\right)_{3(s)} \tag{4}$$

The treatment of wastewater from refineries using the electrocoagulation method and various electrode configurations has been considered the target of several investigations. Abdelwahab et al. [26] explored an electrocoagulation process for the removal of phenol from waste effluent of the oil refinery using a cell with a horizontal aluminum screen anode and a horizontally oriented cathode of aluminum. It was found that at a certain current density, using an anode composed from closely packed Al screens, is more effective than single screen anode. As a main conclusion from such work using aluminum electrodes make the electrocoagulation of phenol promising process. Saeedi and Fahlyani [27] have treated gas refinery oily wastewater treatment by electrocoagulation using aluminum parallel plate electrodes. It was obtained 97% chemical oxygen demand (COD) at the optimum operational conditions. The main conclusion of this research is that the specific electrical energy consumption could be reduced from 19.48 to 11.057 kWh(kg·$\mathrm{COD_{removal}}$)$^{-1}$ using $\mathrm{Na_2SO_4}$ as a supporting electrolyte. El-Naas et al. [28] have analyzed the sulfate removal and COD from the wastewater petroleum refinery's wastewater via electrocoagulation using three electrode types: stainless steel, iron, and aluminum plates. The experimental results of this investigation showed that the utilization of aluminum, as anode and cathode, was the most efficient arrangement in the reduction of both contaminants. In addition, it was concluded that electrocoagulation could be considered as a reliable technique for the pretreatment of heavily contaminated petroleum refinery wastewater. In further investigation, El-Naas et al. [29] evaluated electrocoagulation as a treatment process for reducing high COD concentrations in petroleum refinery wastewater. The experimental work was conducted in continuous mode using an electrocoagulation reactor with aluminum electrodes. It was clearly showed that the reduction of COD content is significantly improved by increasing the current density and decreasing the flow rate. Safari et al. [30] have studied COD and diesel removal from oily wastewater using electrocoagulation. Laboratory tests have been carried out in a 2-l reactor using electrodes of Al and Fe. The highest removal efficiency (COD removal of 99.1%) was observed under the following conditions: pH 7, 40 min, 10.5 V, NaCl concentration of 0.5 g/L, and diesel concentration of 3,500 mg/L. The consumption of energy was estimated to be 6.47 kWh/m^3. The outcomes revealed that the electrocoagulation is a viable method for treatment of heavily contaminated petroleum refinery wastewater. Ibrahim et al. [31] used a batch reactor to treat the oily effluent by electrocoagulation. This research evaluates the influence of the electrode type on electrocoagulation efficiency using parallel plates of mild steel and aluminum as anodes and stainless steel as cathodes. Using mild steel as anode offered maximum percentage removal of COD of 94% under optimum experimental conditions of pH 6.7, current density 6 mA/cm^2, and electrolysis time 40 min. Ibrahim et al. [32] studied the performance of a tubular electrochemical reactor (TER) with a cylindrical mesh electrode for wastewater treatment. A positive influence of the mesh electrode on the flow dynamic behavior of reactor has been obtained. At the most of previous work, no tubular electrochemical reactor (TER) configuration was

employed composed from concentric electrodes with spiral design of the inner meanwhile, parallel plate configurations were used in most prior classical EC operations.

In wastewaters' electrochemical treatment, multiple electrochemical reactor configurations were used. These involve the traditional stack cell, parallel plate reactor, flow cell with mesh anode, rotating disc reactor, tubular electrochemical reactor (TER), and three-dimensional electrodes [33]. Designing and selecting an appropriate electrochemical reactor are essential in an electrochemical process, as the reactor shape affects mass transfer, the reactor's efficiency and process yield [34].

In this work, for the first time, a new design of TER based on a central spiral rode anode surrounded by a hollow cylindrical cathode was utilized to treat petroleum refinery wastewater by an electrocoagulation process. This configuration was not adopted previously, which is the base of the novelty of the present work. Additionally, a batch recycling process was employed to ensure the safe management of waste. The electrodes are made of aluminum to ensure long-term stability since it's more durable, inexpensive and rust-proof. As a coagulant, aluminum generates useful cations (Al^{3+}) [35]. The experimental design depends on the response surface methodology (RSM) that applied to investigate the optimum operating conditions and analyze all parameters simultaneously. Consequently, this work aims to analyze the activity of a novel tubular electrochemical reactor with a spiral design of anode to remove COD from wastewater by an electrocoagulation process. The influences of various operating parameters like current density, pH, NaCl addition and flow rate were also studied using (RSM).

2. Experimental work

2.1. Material and apparatus

A quantity of 120 L of wastewater has been collected from the discharge point at the Al-Samawa petroleum refinery plant in Iraq and then kept at a temperature of 4°C until use. Table 1 displays the properties of the Al-Samawa petroleum refinery wastewater. The conductivity of raw water is 1.1 mS/cm, and due to the law of effluent conductivity, 0.035 mol/L of Na_2SO_4 was added as a supporting electrolyte.

The electrochemical system is shown schematically in Fig. 1. It consists of a tubular electrochemical cell, 5 L capacity Perspex reservoirs for the wastewater, recirculation pumps (GRANDFAR: X15GR-10), and a flow meter with a flow range from 0.5 to 7 L/min for controlling the electrolyte flow rate. This arrangement enables wastewater recirculation through the electrochemical reactor in a batch recycle mode.

The tubular electrochemical reactor is composed of the cell body, and both are made from Teflon. The cell body is 140 mm long, with an internal diameter of 100 mm and an outer diameter of 110 mm. It is closed from the bottom and has a 10-mm diameter entry section on the body's lateral side, near the bottom. A flange with an interior diameter of 100 mm, an outer diameter of 150 mm, a thickness of 10 mm, and four holes of 5 mm are used to link the body cell at the top to secure the body to the cover. An outlet portion having a diameter of 10 mm is located on the lateral side below the flange of the cell body. The cover has an outside diameter of 150 mm, and a thickness of 10 mm, provided with a hole to join the anode and four holes of 5 mm for fixing the cover with the cell body via four bolts and nuts. In this study, a concentric electrode arrangement-based system is designed. The cathode is a tubular 316 stainless steel with dimensions of 99 mm outer diameter, 100 mm length, and 3 mm thickness. It is fixed inside the cell body via a bolt and nut at the centre of its length. The stainless steel 316-AISI chemical composition was found to be (in wt.%): Cr-16.7, Ni-12.2, Mo-2.1, Mn-1.32, Si-0.56, P-0.03, C-0.022, S-0.012, Cu-0.26, (Fe = balance). A spiral aluminum rode is used as a new design of anode. It has an outside diameter of 60 mm and a length of 125 mm. It is drilled along its length in a spiral

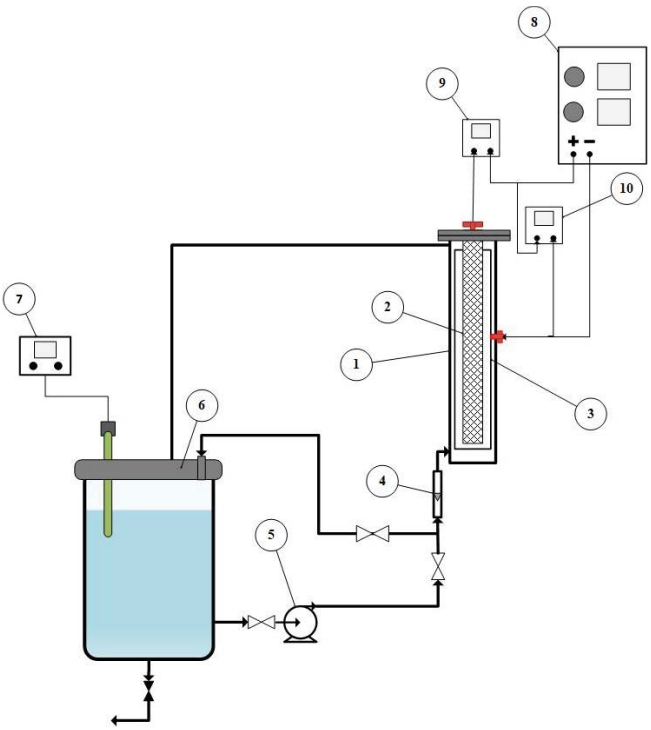

Fig. 1. Electrochemical system's diagram. (1) Cell body, (2) anode, (3) cathode, (4) flow meter, (5) pump, (6) reservoir, (7) pH-meter, (8) power supply, (9) Ammeter, and (10) voltmeter.

Table 1
Wastewater properties of the Al-Samawa petroleum refinery

Parameter	Value
COD, mg/L	563
pH	8.4
Total dissolved solids, mg/L	1,100
Cl^-, mg/L	780
SO_4^{2-}, mg/L	350
Turbidity, NTU	179
Oil content, mg/L	1,677
Conductivity, mS/cm	1.1

fashion with a cavity of 5mm length and 5 mm width. This design makes the electrolyte flow along the lateral surface of the anode in a spiral movement. The anode-to-cathode distance is fixed at 15 mm. The schematic illustration of a tubular electrochemical reactor is shown in Fig. 2.

Before starting each experiment, the Al electrode was cleaned using sodium hypochlorite solution, rinsed many times with distilled water, and dried in the oven at 100°C for 2 h [36].

During each run, a digital power supply with a range (0–30 V), (0–5 A) The utilized type (UNI-T, UTP1305) was to provide constant current and to obtain the required combining conditions; a solution was mixed with a magnetic stirrer at a rotation value (500 rpm) for each experiment. After adding the necessary quantity of NaCl (when required), the pH was adjusted using either 1 M HCl or 1 M NaOH while mixing was continuing at the same rotational speed. The solution was then placed in the reservoir and circulated through the cell at a constant flow rate. The pH adjustment was performed using a digital pH meter (HM Digital, Inc. PH-200). All tests were conducted at a fixed temperature of 25°C ± 2°C.

Based on Eq. (5), the removal efficiency of COD was evaluated [37]:

$$\mathrm{RE\%} = \frac{\mathrm{COD}_i - \mathrm{COD}_f}{\mathrm{COD}_i} \times 100 \tag{5}$$

COD_i indicates the initial COD, COD_f indicates the final COD, and RE% denotes the removal efficiency of COD.

The energy used throughout the process equals the amount of COD that must be digested per kilogram. Specific energy consumption (SEC) may be measured in (kWh/kg·COD) using Eq. (6) [37]:

$$\mathrm{SEC} = \frac{E \times I \times 1000}{\left(\mathrm{COD}_i - \mathrm{COD}_f\right) V} \tag{6}$$

where SEC refers to the specific energy consumption (kWh/kg·COD), *E*: acts the applied cell voltage (V), *t*: acts as the electrolysis time (h), *I*: acts as the current (A), *V*: acts as the effluent volume (L).

2.2. Design of experiments

Mathematical and statistical techniques for optimizing the operational circumstances of response are affected by numerous operating factors of the process from the response surface methodology (RSM). In this work, (3-level, 4-factor) Box–Behnken design (BBD), one of the best designs used in RSM, was adopted as an experimental design to satisfy and examine the process variables that affected COD removal. Four process parameters are involved, and considered as process factors in the BBD, while RE% is taken as a response. The process factors scales were coded as (–1 (low level)), (0 (middle or central point)) and (1 (high level)) [38]. Table 2 shows the process parameters with their chosen levels.

The number of runs (*N*) needed to finish a Box–Behnken design is estimated using the following equation [38]:

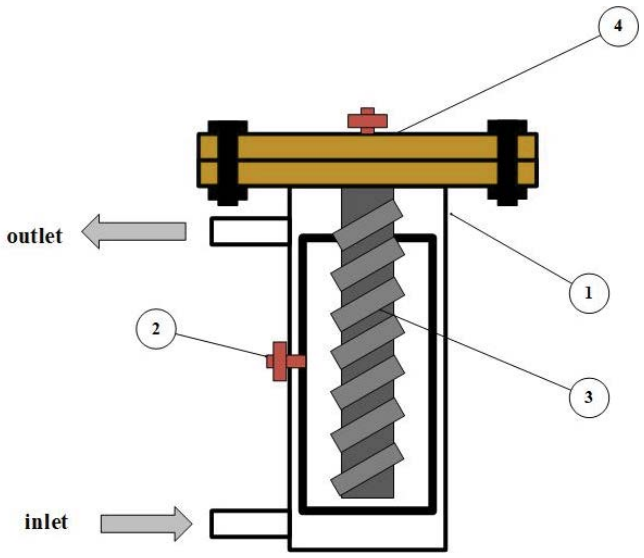

Fig. 2. Electrochemical cell's diagram. (1) Cell body, (2) cathode, (3) anode, and (4) cell cover.

$$\mathrm{N} = 2k\left(k-1\right) + \mathrm{cp} \tag{7}$$

where *k* denotes the number of process variables while cp: denotes the central point's repeated number. Based on Eq. (7), 27 runs were achieved for estimating the impacts of the process factors on the RE%. Table 3 shows the BBD that has been suggested for this study.

Depending on BBD, a second-order polynomial model can be used, with the following equation describing how the interaction terms fit with the experimental results [38]:

$$Y = a_0 + \sum a_i x_i + \sum a_{ii} x_i^2 + \sum a_{ij} x_i x_j \tag{8}$$

where *Y* acts as the response (RE), (*i*) and (*j*) denotes the index numbers for patterns, a_0: intercept term, x_1, x_2 … x_k are the process factors. a_i: the first-order main effect, a_{ii}: the second-order main effect, and a_{ij} acts as the influence of interaction. The regression coefficient (R^2) was evaluated after the inferential analysis to verify that the model fit was appropriate.

3. Results and discussion

3.1. Statistical analysis

As a first step, the time of electrolysis for achieving all the experiments of BBD was determined by performing an experiment based on the following conditions: current density = 26 mA/cm^2, pH = 6.5, NaCl addition = 1 g/L, flow rate = 4 L/min. The results are illustrated in Table 4. The selection of these values was based on previous studies on this topic.

It was evident that an electrolysis time of 60 is sufficient for adopting in the experimental design as it provides RE% of 60%, that is, higher than 50% that is suitable for making a clear comparison of the effect of process variables based on RSM.

Table 2
Refinery wastewater treatment process variables and their values

Process variables	Range		
Codes	Low (–1)	Middle (0)	High (+1)
(X_1): current density (mA/cm^2)	4	15	26
(X_2): pH	3	6.5	10
(X_3): NaCl (g/L)	0	1	2
(X_4): flow rate (L/min)	1	2.5	4

Table 3
Experimental design by Box–Behnken

Run	Blocks	Coded values				Real values			
		x_1	x_2	x_3	x_4	Current density (mA/cm^2) X_1	pH X_2	NaCl addition (g/L), X_3	Flow rate (L/min) X_4
1	1	–1	–1	0	0	4	3	1	2.5
2	1	1	–1	0	0	26	3	1	2.5
3	1	–1	1	0	0	4	10	1	2.5
4	1	1	1	0	0	26	10	1	2.5
5	1	0	0	–1	–1	15	6.5	0	1
6	1	0	0	1	–1	15	6.5	2	1
7	1	0	0	–1	1	15	6.5	0	4
8	1	0	0	1	1	15	6.5	2	4
9	1	–1	0	0	–1	4	6.5	1	1
10	1	1	0	0	–1	26	6.5	1	1
11	1	–1	0	0	1	4	6.5	1	4
12	1	1	0	0	1	26	6.5	1	4
13	1	0	–1	–1	0	15	3	0	2.5
14	1	0	1	–1	0	15	10	0	2.5
15	1	0	–1	1	0	15	3	2	2.5
16	1	0	1	1	0	15	10	2	2.5
17	1	–1	0	–1	0	4	6.5	0	2.5
18	1	1	0	–1	0	26	6.5	0	2.5
19	1	–1	0	1	0	4	6.5	2	2.5
20	1	1	0	1	0	26	6.5	2	2.5
21	1	0	–1	0	–1	15	3	1	1
22	1	0	1	0	–1	15	10	1	1
23	1	0	–1	0	1	15	3	1	4
24	1	0	1	0	1	15	10	1	4
25	1	0	0	0	0	15	6.5	1	2.5
26	1	0	0	0	0	15	6.5	1	2.5
27	1	0	0	0	0	15	6.5	1	2.5

27 runs were carried out at various process sets to study the expected impacts of the operation parameters on removal efficiency. Table 5 shows the practical results of RE% gained at 60 min and the predicted values based on the model equation. Specific energy consumption (SEC) is also outlined in the table.

It was observed that RE% is in the range of 45%–70.1%. The specific energy consumption is in the range of

1.54–48.16 kWh/kg·COD. The difference among the central points in the design is less than 2%, confirming good reproducibility of results. Using Minitab-17 Software, based on analysing the results of RE%, as indicated in Eq. (9) below, a quadratic model in terms of absolute values of system factors was developed, which connects RE% with process factors:

$$\begin{aligned}RE\% = {} & 34.76 + 0.591X_1 + 2.69X_2 + 19.78X_3 + 2.54X_4 \\ & - 0.01280(X_1)^2 - 0.2870(X_2)^2 - 9.683(X_3)^2 - 1.626(X_4)^2 \\ & + 0.0346X_1X_2 + 0.0170X_1X_3 + 0.0477X_1X_4 + 0.137X_2X_3 \\ & + 0.380X_2X_4 + 0.167X_3X_4 \end{aligned} \quad (9)$$

Table 4
COD variation with time

COD (ppm)	Time (min)
563	0
380	30
270	60
180	90
140	120

where X_1, X_2, X_3, X_4 acts process variables while X_1X_2, X_1X_3, X_1X_4, X_2X_3, X_2X_4 and X_3X_4 acts the interaction influence among these variables $(X_1)^2$, $(X_2)^2$, $(X_3)^2$, and $(X_4)^2$ represent a measurement of the fundamental impact of these factors. Synergistic and antagonistic impacts are shown by the (+, −) signs in front of the variables and their interaction terms [39].

Table 6 explains the analysis of variance (ANOVA) data of the response model in which: DF denote the degree of freedom, Seq. SS denote the sum of the square, Adj. SS represent the adjusted sum of the square, Adj. MS symbolize the adjusted mean of the square and Contr.% perform contribution for each parameter. The model's capacity was examined using Fisher's (*F*-test) and (*P*-test), where a high Fisher value indicates that the regression equation can match the diversity's maximum limits. The (*P*-value) is utilized to determine if (*F*) has a significant value that is reasonable to distinguish the statistical importance of the model. 95% of the variability of the model could be discussed when its *P*-value is lower than 5% [40].

According to Table 6, the quadratic model is essential with an *F*-value of 23.88 and a confidence level above 95% (*P*-value equal to 0.0001). The lack-of-fit test can be utilized

Table 5
Results of experimental of BBD to remove COD

Run order	Blocks	Current density (mA/cm²)	pH	NaCl addition (g/L)	Flow rate (L/min)	*E* (Volt)	RE%		Al consumption (g/L)	SEC (kWh/kg·COD)
							Actual	Predicted		
1	1	4	3	1	2.5	2.50	51.72	53.31333	1.330	2.11
2	1	26	3	1	2.5	8.15	59.27	63.15667	0.666	34.75
3	1	4	10	1	2.5	2.83	57.12	54.58333	0.833	1.92
4	1	26	10	1	2.5	8.175	70.00	69.75667	0.833	30.21
5	1	15	6.5	0	1	6.40	53.00	53.555	0.133	18.66
6	1	15	6.5	2	1	5.03	56.00	57.01667	0.103	13.84
7	1	15	6.5	0	4	6.80	46.00	46.33333	0.333	24.27
8	1	15	6.5	2	4	5.25	50.00	50.795	0.333	15.16
9	1	4	6.5	1	1	2.23	57.74	57.95417	0.500	1.54
10	1	26	6.5	1	1	9.64	70.10	68.8875	0.100	34.33
11	1	4	6.5	1	4	2.45	49.49	49.6575	0.033	1.90
12	1	26	6.5	1	4	10.80	65.00	63.74083	0.100	44.42
13	1	15	3	0	2.5	7.40	50.95	48.59917	0.500	20.92
14	1	15	10	0	2.5	6.29	51.22	51.57417	0.500	17.67
15	1	15	3	2	2.5	5.98	53.00	51.60083	0.660	16.18
16	1	15	10	2	2.5	6.00	55.19	56.49583	0.660	15.83
17	1	4	6.5	0	2.5	3.20	45.00	45.9875	0.500	2.80
18	1	26	6.5	0	2.5	11.20	58.00	58.12083	1.160	48.16
19	1	4	6.5	2	2.5	2.51	50.00	49.57417	0.330	1.80
20	1	26	6.5	2	2.5	8.85	63.75	62.4575	0.660	37.20
21	1	15	3	1	1	6.69	62.48	61.48083	0.330	14.64
22	1	15	10	1	1	6.10	61.00	61.42583	0.500	14.34
23	1	15	3	1	4	5.30	51.50	50.76917	0.167	14.80
24	1	15	10	1	4	5.50	58.00	58.69417	0.167	13.45
25	1	15	6.5	1	2.5	7.96	64.50	65.26667	0.133	17.00
26	1	15	6.5	1	2.5	8.00	65.30	65.26667	0.140	17.50
27	1	15	6.5	1	2.5	7.90	66.00	65.26667	0.135	17.20

Table 6
ANOVA for COD elimination

Source	DF	Seq. SS	Cr. (%)	Adj. SS	Adj. MS	*F*-value	*P*-value
Model	14	1,248.84	96.53	1,248.84	89.203	23.88	0.0001
Linear	4	698.45	53.99	698.45	174.614	46.74	0.0001
X_1	1	469.38	36.28	469.38	469.375	125.64	0.0001
X_2	1	46.45	3.59	46.45	46.453	12.43	0.001
X_3	1	47.08	3.64	47.08	47.084	12.60	0.001
X_4	1	135.54	10.48	135.54	135.542	36.28	0.0001
Square	4	523.57	40.47	523.57	130.893	35.04	0.0001
X_1X_1	1	22.16	1.71	12.79	12.786	3.42	0.089
X_2X_2	1	0.21	0.02	65.93	65.926	17.65	0.001
X_3X_3	1	429.82	33.23	500.09	500.090	133.86	0.0001
X_4X_4	1	71.38	5.52	71.38	71.378	19.11	0.001
2-Way interaction	6	26.82	2.07	26.82	4.469	1.20	0.371
X_1X_2	1	7.10	0.55	7.10	7.102	1.90	0.193
X_1X_3	1	0.14	0.01	0.14	0.141	0.04	0.849
X_1X_4	1	2.48	0.19	2.48	2.481	0.66	0.431
X_2X_3	1	0.92	0.07	0.92	0.922	0.25	0.628
X_2X_4	1	15.92	1.23	15.92	15.920	4.26	0.061
X_3X_4	1	0.25	0.02	0.25	0.250	0.07	0.800
Error	12	44.83	3.47	44.83	3.736		
Lack-of-fit	10	43.71	3.38	43.71	4.371	7.76	0.119
Pure error	2	1.13	0.09	1.13	0.563		
Total	26	1,293.67	100				
Summary model	S	R^2	R^2 (Adj.)	PRESS	R^2 (Pred.)		
	1.93287	96.53	92.49	254.277	80.34		

to see if the chosen model is acceptable for describing the data or if a more extensive model is required [25]. The *P*-value for lack-of-fit in the current work is equal to 0.119, which is larger than 0.05, demonstrating that the lack of model fit was not statically significant when compared to the pure error [25]. As a result, the model can acquire reasonable predictions matching the response values. The R^2, Adj. R^2, Pred. R^2 values in this study were assessed to be 96.53%, 92.49%, and 80.34%, respectively, confirming the consistency of the model-predicted and experimental values [33].

It is clear from Table 6 that among every factor, current density (X_1) was the most significant factor effect on RE% with a contribution percentage equal to 36.28%, which indicates the role of current density on the degradation of the organic compound during the electrocoagulation. With a percentage contribution (10.48%), the effect of flow rate (X_4) is the second most important factor. This interesting effect of flow rate results from the spiral design of the anode that gives more retention time in the cell leading to a higher generation of $Al(OH)_3$. pH has a considerable effect on RE% with a percentage of contribution of 3.59% and shares the same effect with the addition of NaCl. Furthermore, the contribution of 2-way interaction impacts, the RE% by about 2.07%, which is very small and could be ignored. The contributions of the Square on the RE% was approximately 40.47% which is significant.

3.2. Influence of operation variables on the COD elimination efficiency

Graphical presentation of quadratic model depend on RSM was employed to knowledge effect of process parameters and their combination on the removal efficiency.

Fig. 3a and b demonstrate the total impacts of current density and NaCl addition on the RE% with pH = 6.5 and a flow rate of 2.5 L/min. Fig. 3a denotes the response surface plot, while Fig. 3b describes the equivalent contour plot.

From Fig. 3a it is clear that the increasing in current density leads to increase RE% over the whole range of NaCl addition. For example, without addition of NaCl, current density increases from 4 to 26 mA/cm^2 and RE% increases from 45% to 58% (Table 5, exp.17 and 18). The same behaviour was observed at NaCl addition of 2 g/L (Table 5, exp.19 and 20).

Increased current accelerates anode dissolution raises the concentration of metal ions in the solution and, as a result, increases the rate at which pollutants are removed from the solution [28]. Coagulation dose rate, bubble size, and flocs development are all influenced by current density in electrocoagulation. These factors may impact COD elimination rates [41,42]. Hence, the current density is considered the most significant parameter in electrocoagulation that governs electron transport and the production of Al^{3+}, leading to $Al(OH)_3$ and bubble density. Such major affecting

function of current densities through removing pollutants from different wastewater has been reported in many studies [29,43,44].

The effect of NaCl addition is less pronounced than current density. For example, at the current density of 4 mA/cm^2, increasing the addition of NaCl from 0 to 2 g/L results in increasing RE% from 45% to 50% (Table 5, exp.17 and 19). The same behavior was observed at higher current density. However, during the increase of NaCl concentration from 0 to 2 g/L, the removal efficiency increases to higher value at NaCl concentration around 1 g/L, then decreases beyond this value as shown in Fig. 3a. Literature surveys have shown that the addition of NaCl has different effects on the electrocoagulation process [27]. It enhances the degradation efficiency and shortens the reaction time because of the reaction between the produced (chlorine/hypochlorite) and the organic molecule. Also, it increases the conductivity of the solution leading to less power consumption [37]. Other benefits of enhancing water conductivity with NaCl include that chloride anions may considerably minimize the harmful effects of different anions, such as $(HCO_3)^-$ ions, on water quality. Similar behavior was observed in previous studies [45,46].

Depending on the results of the contour plot, it is obvious that RE% ≥ 70% could be gained within a limited region in which NaCl addition is (1–1.1 g/L), and the current density is within 26 mA/cm^2.

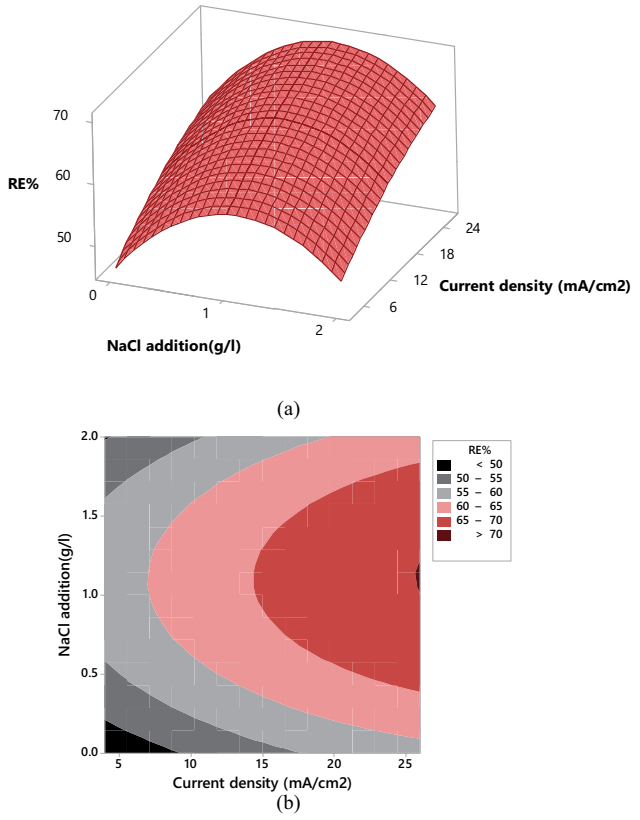

Fig. 3. Plot of response surface (a) plot of contour and (b) for the impact of current density and NaCl concentration on the activity of COD elimination. Hold values: pH = 6.5 and flow rate = 2.5 L/min.

Fig. 4a and b demonstrate the total impacts of current density and pH on the RE% with sodium chloride addition of 1 g/L and flow rate of 2.5 L/min. Fig. 3a denotes the response surface plot, while Fig. 3b describes the equivalent contour plot.

Fig. 4a displays that RE% increases with increasing current density at the whole range of pH. Meanwhile, the opposite effect was observed by pH, where increasing pH from 4 to 8 leads to a drastic increasing in RE% while beyond 8, the RE% is decreased. Electrochemical and chemical processes are affected by the pH of the solution. By the amphoteric chart of aluminum hydroxide $Al(OH)_3$, which precipitates at pH 6–7 and rises in solubility as the solution gets more acidic, the decline in COD reduction at low pH values is seen [43,44,47]. More $Al(OH)_3$ precipitation results in greater removal of colloidal particles from the solution. With regard to pH ≥ 10, $Al(OH)_4^-$ will be prevalent, they have weak coagulation performances so the coagulation effect rapidly reduces [48]. The cathodic process in Eq. (3), which occurs during electrocoagulation, raises the pH of the electrolyte solutions [49].

Similar behavior regarding to the effect of pH was observed by [27,32,45]. According to the plot of contour results, it is evident that RE% ≥ 70% could be achieved within a limited region in which pH is within (6.5–9.5) and current density is within 22–26 mA/cm^2.

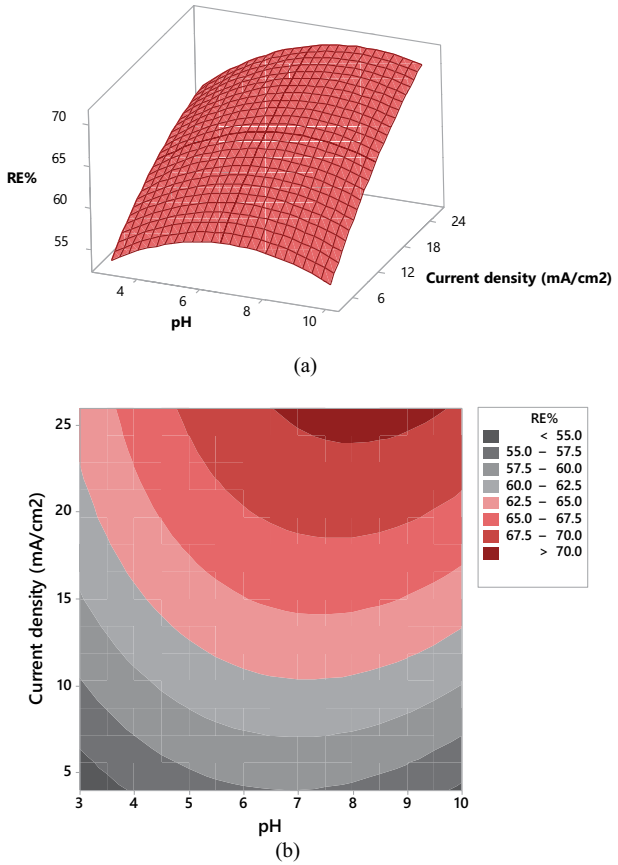

Fig. 4. Plot of response surface (a) contour plot and (b) for the impact of current density and pH on the removal efficiency. Hold values: NaCl addition = 1 g/L and flow rate = 2.5 L/min.

Fig. 5a and b demonstrate the combined influences of flow rate and current density on the RE% at pH value equal to 6.5 and sodium chloride addition of 1 g/L. Fig. 5a denotes the plot of the response surface while, Fig. 5b demonstrates the plot of equivalent contour.

Fig. 5a shows RE% increases with increasing current density over the whole range of flow rate. The most significant point in this figure is the role of flow rate on the RE%. It was observed that raising the flow rate from 1 to 2.5 L/min has no significant effect on RE% however, beyond 2.5 L/min, there is a decreasing in the RE% to reach 49.49% at a current density of 4 mA/cm^2 (Table 5, exp.11). This is to be predicted, since faster flow rates lead to a shorter retention period, resulting in less time for contaminants to react with $Al(OH)_3$ in the reactor. Besides, previous studies confirmed that a higher in flow rate reduces the opportunity for electrocoagulation [50,51]. Decreasing flow rate also contributes in reducing turbulence in the cell, favouring floc formation and flotation [52]. Similar observations regarding the effect of flow rate were found in previous studies [45,46,52]. Depending on contour plot results, it is evident that RE% ≥ 70% might be achieved within a small region in which flow rate is within (1.5–2.5 L/min), and current density is within 23–26 mA/cm^2.

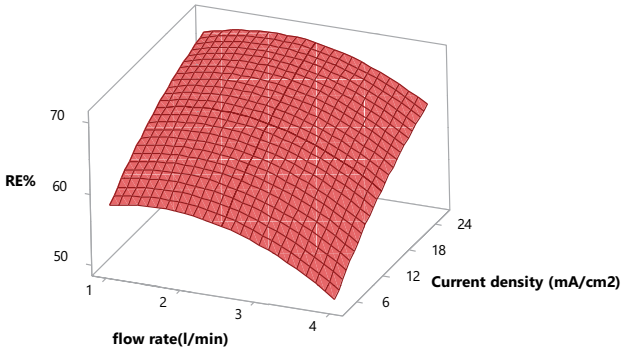

(a)

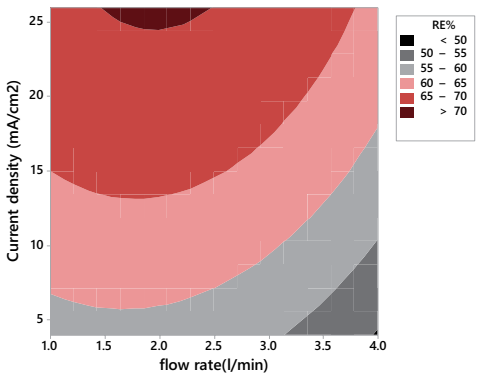

(b)

Fig. 5. Plot of response surface (a) plot of contour and (b) for the impact of current density and flow rate on the efficiency of COD elimination. Hold values: pH = 6.5 and NaCl = 1 g/L.

3.3. Confirmation test and the optimization

The purpose of any optimization process is to achieve a higher response value. As a result, RE% was selected as the maximum, with a weight of 1.0. To accomplish optimization, Minitab-17 Software's response optimizer was used. Results of optimization are explained in Table 7 with the optimal desirability function (DF) of (1). Table 8 displays two experiments performed based on the optimized factors to confirm the optimization results. A COD elimination efficiency (average value) of 72.73% was achieved after 60 min of electrolysis, which is within the range of the best values obtained from ideal outcomes (Table 7). As a result, a Box–Behnken design with DF may be used to optimize the percentage of RE produced by the EC process by employing TER with a spiral aluminum anode. Table 9 compares the properties of wastewater treated with the new TER design to the characteristics of not treated effluent. It was clear that treated effluent has improved features with RE% of 73.36% and a final COD value of 150 ppm near the allowable limits for discharging effluents to the river achieving more than 93% of turbidity and more than 97% oil content removal.

3.4. Estimation of the operating cost for electrocoagulation

The total operating cost of the electrocoagulation process consists of materials, electrical energy, labor, maintenance, sludge dewatering, disposal, and fixed costs [53]. However, various costs are not included in the calculation portion and are assumed to be constant, such as sludge dewatering costs, labor, maintenance, and disposal costs [54]. The operating cost can be estimated using the following equation [55]:

$$\text{operating cost} = aC_{\text{energy}} + bC_{\text{electrode}} \tag{10}$$

where a is electrical energy price in \$/kWh, b is electrode material price in \$/kg, C_{energy} and $C_{\text{electrode}}$ are energy consumption (kWh/m^3) and electrode consumption (kg/m^3), respectively.

According to Iraqi Electric Power Agency, the amount of tariff paid for electrical energy on December 2021 was 0.041\$/kWh [56]. The price of Al in Iraq is 1.713\$/kg [57].

Based on Table 8 run (2):

SEC = 30.61 kWh/kg·COD × 0.413 kg/m^3 = 12.642 kWh/m^3

Al consumption = 0.973kg/m^3

Hence the operating cost is:

Operating cost = 0.041 \$/kWh × 12.642 kWh/m^3 + 1.713 \$/kg × 0.973 kg/m^3

Operating cost = 2.185\$/m^3

The operating cost of the present system is lower than those reported by Safari et al. [30]. However, the operating cost of the present system is higher than those mentioned by Giwa et al. [58] in terms of treating petroleum refinery wastewater by EC. On the other hand, the initial COD was 150 ppm which is lower than the value that obtain in the present work (563 ppm). Consequently, the present system is considered better than that adopted by Giwa et al. [58]. Concerning the operating cost of treatment

Table 7
Best values of process factors for improving COD removal efficiency

Response	Goal		Lower	Target	Upper		Weight	Importance
RE (%)	Maximum		45	70.1			1	1
Solution: parameters				Results				
Current density (mA/cm^2)	pH	NaCl conc. (g/L)	Flow rate (L/min)	RE (%) fit	DF	SE fit	(95%) CI	(95%) PI
26	7.94	1.111	2.15	71.0816	1.0	1.08	(68.73, 73.43)	(66.26, 75.90)

Table 8
Confirmation runs based on optimum conditions

Run	Current density (mA/cm^2)	pH	NaCl (g/L)	Flow rate (L/min)	E (Volt)	COD (ppm)		RE (%)		Al consumption (g/L)	SEC (kWh/kg·COD)
						Initial	Final				
1	26	7.9	1.1	2.0	8.15	580	161	72.1	72.73	0.961	31.5
2	26	7.9	1.1	2.0	8.1	563	150	73.36		0.973	30.61

Table 9
Properties of the treated effluent vs. wastewater effluent

Parameter Effluent	COD (ppm)	Turbidity (NTU)	Oil content (ppm)	SO_4^{-2} (mg/L)	Cl^- (mg/L)
Raw effluent	563	179	1677	350	780
Treated effluent	150 (73.36%)	11.2 (93.74%)	41.7 (97.51%)	1300	630

of domestic wastewater by Ozyonar and Karagozoglu [59] and Treatment of Boron from Aqueous by Deniz and Akarsu [55], the operating cost of the present system is considered lower and economical.

3.5. Characterization of the sludge

The sludge composition from the aluminum anode was analyzed by energy-dispersive X-ray spectroscopy (EDX), as shown in Fig. 6 and Table 10. The EDX analysis confirmed the existence of organic and inorganic pollutants in the sludge. Elements as O, C, Zn, Mg, Mo, and Sn were adsorbed on $Al(OH)_{3(s)}$ surface. These flocs were destabilized and precipitated [32]. Al detected in the sludge comes from the Al electrode. The low detection of C levels in sludge could result from converting most of C to CO_2 gas during the bubble formation in the EC process [31]. The high level of O reveals the formation of $Al(OH)_3$ as a significant constituent in the sludge.

The structure of sludge after electrocoagulation was examined by scanning electron microscopy (SEM), as shown in Fig. 7. Experimental results demonstrate that EC sludge employing Al settles at the reservoir's bottom. The SEM image shows that the sludge particle size is large, about 1 μm. Results also show that the sludge is composed of discontinuous layers of materials with many void spaces and hollows [31].

The Fourier-transform infrared spectroscopy (FTIR) analysis was carried out to identify the functional groups in the sludge, as shown in Fig. 8. The strong peak at 3,421.72 cm^{-1} represents the O–H stretching of alcohol. Peaks at 2,924.09 and 2,854.65 cm^{-1} are related to the C–H stretching of alkene. Another peak at 2,569.19 cm^{-1} represents the S–H stretching of a sulfur compound such as thiol. Peak of 2,156.42 cm^{-1} relates to C=C=O stretching of ketone, while 1,643.36 cm^{-1} means C=C stretching of alkene. C–O stretching of aliphatic ether is located at 1,091.71 cm^{-1}, while C–N stretching of amine is located at 1,014.56 cm^{-1}. The peak at 586.36 cm^{-1} could be attributed to the C–I stretching of a hollow compound. In conclusion, the effluent generated from petroleum refinery wastewater contains many organic compounds and sulfur compounds. A similar observation was found in previous works [32].

4. Conclusions

A tubular electrochemical reactor operated in a batch recycle mode and made from a stainless steel cylindrical cathode with aluminum spiral rode as an anode was examined for treating petroleum refinery wastewater collected from the Al-Samawa refinery plant in Iraq. Optimization of the influences of process variables, namely current density, NaCl addition, pH and flow rate on the removal of COD using RSM, was performed. A quadratic model equation was developed to estimate the interactions between the response (RE%) and its independent variables. The reliability of the quadratic model was confirmed by its R^2 value (96.53%) to be significant. Results show that the best achieved conditions are: current density equal to 26 A/cm^2, NaCl concentration equal to 1.1 g/L, pH of 7.9, and flow rate

equal to 2 L/min, in which efficiency of COD elimination of 73.36%, with specific energy consumption of 30.61 kWh/kg·COD. Besides, results show that the most significant factor is the current density on RE%, followed by flow rate. In addition, the effect of flow rate is vital where higher removal of COD occurred at low flow rate value, resulting in high effluent retention time fluent on the surface of the anode due to the spiral design adopted in this work. It's worthwhile to investigate the performance of such a new design for the electrocoagulation process in the treatment of other wastewater, such as pharmaceutical effluent.

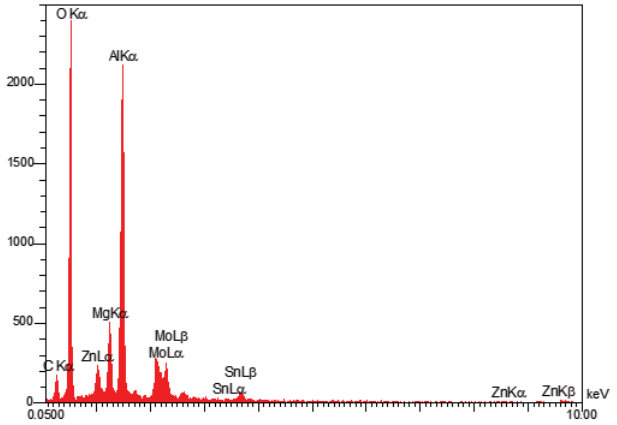

Fig. 6. Energy-dispersive X-ray analysis of sludge produced at the optimum conditions of electrocoagulation using Al anode.

Table 10
EDX elements analysis

Element	W%	A%
C	12.89	19.25
O	59.32	66.48
Mg	3.55	2.62
Al	14.86	9.87
Zn	0.42	0.12
Mo	8.83	1.65
Sn	0.13	0.02

Acknowledgments

The authors are grateful for the Al-Samawa petroleum refinery plant's staff's support and technical assistance in completing this study.

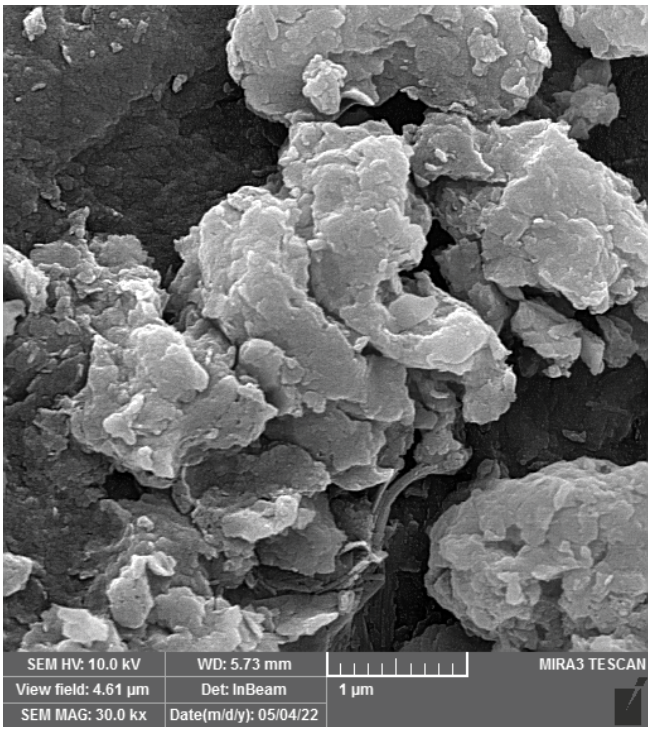

Fig. 7. SEM image of sludge produced at the optimum conditions of electrocoagulation using Al anode.

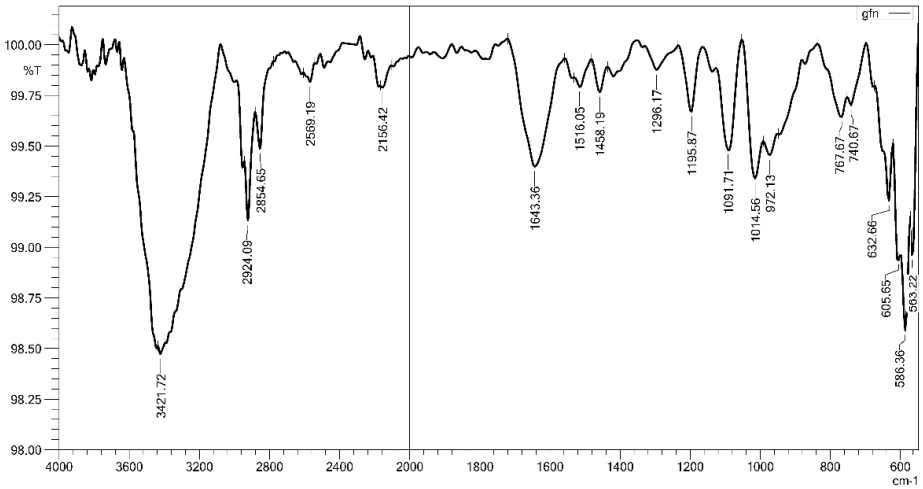

Fig. 8. FTIR spectrum of sludge produced at the optimum conditions of electrocoagulation using Al anode.

Symbols

A	—	Electrical energy price, $/kWh
b	—	Electrode material price, $/kg
COD_i	—	Initial value of COD, ppm
COD_f	—	Final value of COD, ppm
RE%	—	Removal efficiency of COD
SEC	—	Specific energy consumption, kWh/kg·COD
E	—	Applied cell voltage, Volt
t	—	Electrolysis time, hr
I	—	Current, Amp
V	—	Effluent volume, L
N	—	Number of runs
k	—	Number of process variables
cp	—	Central points repeated number
Y	—	Response, RE
i, j	—	Index numbers for patterns
a_0	—	Intercept term
a_i	—	First-order main effect
a_{ii}	—	Second-order main effect
a_{ij}	—	Influence of interaction
x_i, x_j, X_1, X_2, X_3, X_4	—	Process factors

References

[1] R. Shpiner, S. Vathi, D.C. Stuckey, Treatment of produced water by waste stabilization ponds: removal of heavy metals, Water Res., 43(2009) 4258–4268.

[2] W.E. Allen, Process water treatment in Canada's oil sands industry: II. A review of emerging technologies, J. Environ. Eng. Sci., 7 (2008) 499–524.

[3] H.I. Mustapha, J.J.A.V. Bruggen, P.N.L. Lens, Vertical subsurface flow constructed wetlands for polishing secondary Kaduna refinery wastewater in Nigeria, Ecol. Eng., 84 (2015) 588–595.

[4] B.H. Diya'uddeen, W.M.A.W. Daud, A.R. Abdul Aziz, Treatment technologies for petroleum refinery effluents: a review, Process Saf. Environ. Prot., 89 (2011) 95–105.

[5] S.E. Agarry, A.O. Durojaiye, R.O. Yusuf, M.O. Aremu, B.O. Solomon, O. Majeed, Biodegradation of phenol in refinery wastewater by pure cultures of *Pseudomonas aeruginosa* NCIB 950 and *Pseudomonas fluorescence* NCIB 3756, Int. J. Environ. Pollut., 32 (2008) 3–11.

[6] U.G. Akpan, E.A. Afolabi, K. Okemini, Modelling and simulation of the effect of effluent from Kaduna refinery and petrochemical company on River Kaduna, AU J. Technol., 12 (2008) 98–106.

[7] M.M. Spacil, J.H. Rodgers Jr., J.W. Castle, C.L.M. Gulde, J.E. Myers, Treatment of Selenium in simulated refinery effluent using a pilot-scale constructed wetland treatment system, Water Air Soil Pollut., 221 (2011) 301–312.

[8] L. Marchand, M. Mench, D.L. Jacob, M.L. Otte, Metal and metalloid removal in constructed wetlands, with emphasis on the importance of plants and standardized measurements: a review, Environ. Pollut., 158 (2010) 3447–3461.

[9] C. Jadia, M. Fulekar, Phytoremediation of heavy metals: recent techniques, Afr. J. Biotechnol., 8 (2009) 921–928.

[10] G. Imfeld, M. Braeckevelt, P. Kuschk, H.H. Richnow, Monitoring and assessing processes of organic chemicals removal in constructed wetlands, Chemosphere, 74 (2009) 349–362.

[11] D.A. Aljuboury, P. Palaniandy, H.B. Abdul Aziz, S. Feroz, Treatment of petroleum wastewater by conventional and new technologies – a review, Global NEST J., 19 (2017) 439–452.

[12] L. Alta, H. Bükgüyüngör, Sulfide removal in petroleum refinery wastewater by chemical precipitation, J. Hazard. Mater., 153 (2008) 462–469.

[13] H. Farajnezhad, P. Gharbani, Coagulation treatment of wastewater in petroleum industry using poly aluminum chloride and ferric chloride, Int. J. Res. Rev. Appl. Sci., 13 (2012) 306–310.

[14] Y. Zenga, C. Yang, J. Zhang, W. Pu, Feasibility investigation of oily wastewater treatment by combination of zinc and PAM in coagulation/flocculation, J. Hazard. Mater., 147 (2007) 991–996.

[15] J.V.F.L. Cavalcanti, C.A.M. Abreu, M.N. Carvalho, M.A.M. Sobrinho, M. Benachour, O.S. Barauna, Removal of effluent from petrochemical wastewater by adsorption using organo-clay, Dr Vivek Patel, ed., Petrochemicals, InTechOpen, 2012, pp. 277–294.

[16] M.H. Al-Malack, Performance of constant-flux immersed UF membrane treating petroleum refinery wastewater, Desal. Water Treat., 57 (2016) 8608–8618.

[17] L. Li, N. Liu, B. McPherson, R. Lee, Influence of counter ions on the reverse osmosis through MFI zeolite membranes: implications for produced water desalination, Desalination, 228 (2008) 217–225.

[18] X. Zhao, Y. Wang, Z. Ye, A.G.L. Borthwick, J. Ni, Oil field wastewater treatment in biological aerated filter by immobilized microorganisms, Process Biochem., 41 (2006) 1475–1483.

[19] K. Rajeshwar, J.G. Ibanez, Environmental Electrochemistry: Fundamentals and Applications in Pollution Abatement, Academic Press, San Diego, California, USA, 1997.

[20] A. Riyanto, A. Hidayatillah, Electrocoagulation of Detergent Wastewater Using Aluminium Wire Netting Electrode (AWNE), Proceeding of International Conference on Research, Implementation and Education of Mathematics and Science, 2014, pp. 151–158.

[21] A. Rehman, M. Kimb, A. Reverberic, B. Fabiano, Operational parameter influence on heavy metal removal from metal plating wastewater by electrocoagulation process, Chem. Eng. Trans., 43 (2015) 2251–2256.

[22] B. Lekhlif, L. Oudrhiri, F. Zidane, P. Drogui, J.F. Blais, Study of the electrocoagulation of electroplating industry wastewaters charged by nickel(II) and chromium(VI), J. Mater. Environ. Sci., 5 (2014) 111–120.

[23] H.G. Attia, Decolorization of direct blue dye by electrocoagulation process, J. Eng. Dev., 17 (2013) 171–181.

[24] A.I. Adeogun, R.B. Balakrishnan, Electrocoagulation removal of anthraquinone dye Alizarin red s from aqueous solution using aluminum electrodes: kinetics, isothermal and thermodynamics studies, J. Electrochem. Sci. Eng., 6 (2016) 199–213.

[25] E. Bazrafshan, L. Mohammadi, A.A. Moghaddam, A.H. Mahvi, Heavy metals removal from aqueous environments by electrocoagulation process– a systematic review, J. Environ. Health Sci. Eng., 13 (2015) 1–16.

[26] O. Abdelwahab, N.K. Amin, E.-S.Z. El-Ashtoukhy, Electrochemical removal of phenol from oil refinery wastewater, J. Hazard. Mater., 163 (2009) 711–716.

[27] M. Saeedi, A.K. Fahlyani, Treatment of oily wastewater of a gas refinery by electrocoagulation using aluminum electrodes, Water Environ. Res., 83 (2011) 255–264.

[28] M.H. El-Naas, S. Al-Zuhair, A. Al-Lobaney, Assessment of electrocoagulation for the treatment of petroleum refinery wastewater, J. Environ. Manage., 91 (2009) 180–185.

[29] M.H. El-Naas, S. Al-Zuhair, A. Al-Lobaney, Treatment of petroleum refinery wastewater by continuous electrocoagulation, Int. J. Eng. Res. Technol., 2 (2013) 2144–2150.

[30] S. Safari, M.A. Aghdam, H.R. Kariminia, Electrocoagulation for COD and diesel removal from oily wastewater, Int. J. Environ. Sci. Technol., 13 (2016) 231–242.

[31] D.S. Ibrahim, N. Sakthipriya, N. Balasubramanian, Electrocoagulation treatment of oily wastewater with sludge analysis, Water Sci. Technol., 66 (2012) 2533–2538.

[32] D.S. Ibrahim, M. Lathalakshmi, A. Muthukrishnaraj, N. Balasubramanian, An alternative treatment process for upgrade of petroleum refinery wastewater using electrocoagulation, Pet. Sci., 10 (2013) 421–430.

[33] D.S. Ibrahim, C. Veerabahu, R. Palani, S. Devi, N. Balasubramanian, Flow dynamics and mass transfer studies in a tubular electrochemical reactor with a mesh electrode, Comput. Fluids, 73 (2013) 97–103.

[34] S.T. Kadhum, G.Y. Alkindi, T.M. Albayati, Remediation of phenolic wastewater implementing nano zerovalent iron as a granular third electrode in an electrochemical reactor, Int. J. Environ. Sci. Technol., 19 (2022) 1383–1392.
[35] Sudibyo, L. Hermida, Suwardi, Application of Taguchi optimization on the cassava starch wastewater electro-coagulation using batch recycle method, AIP Conf. Proc., 1904 (2017) 020006-1–020006-8, doi: 10.1063/1.5011863.
[36] T. Tyborski, Alkaline Cleaner for Cleaning Aluminum Surfaces, U.S. Patent No. 9,222,176, U.S. Patent and Trademark Office, Washington, D.C., 2015.
[37] S.S. Alkurdi, A.H. Abbar, Removal of COD from petroleum refinery wastewater by electro-coagulation process using SS/Al electrodes, IOP Conf. Ser.: Mater. Sci. Eng., 870 (2020) 012052, doi: 10.1088/1757-899X/870/1/012052.
[38] M. Evans, Optimization of Manufacturing Processes: A Response Surface Approach, Carlton House Terrace, London, 2003.
[39] E. Ahmadi, B. Shokri, A. Mesdaghinia, R. Nabizadeh, M. Reza Khani, S. Yousefzadeh, M. Salehi, K. Yaghmaeian, Synergistic effects of α-FeO_3-TiO_2 and $Na_2S_2O_8$ on the performance of a non-thermal plasma reactor as a novel catalytic oxidation process for dimethyl phthalate degradation, Sep. Purif. Technol., 250 (2020) 117185, doi: 10.1016/j.seppur.2020.117185.
[40] J. Segurola, N.S. Allen, M. Edge, A.M. Mahon, Design of eutectic photoinitiator blends for UV/visible curable acrylated printing inks and coatings, Prog. Org. Coat., 37 (1999) 23–37.
[41] N. Adhoum, L. Monser, Decolourization and removal of phenolic compounds from olive mill wastewater by electrocoagulation, Chem. Eng. Process, 43 (2004) 1281–1287.
[42] T. Kim, C. Park, J. Lee, E. Shin, S. Kim, Pilot scale treatment of textile wastewater by combined process (fluidized biofilm process–chemical coagulation–electrochemical oxidation), Water Res., 36 (2002) 3979–3988.
[43] K. Bensadok, S. Benammar, F. Lapicque, G. Nezzal, Electrocoagulation of cutting oil emulsions using aluminium plate electrodes, J. Hazard. Mater., 152 (2008) 423–430.
[44] A.E. Yilmaz, R. Boncukcuoglu, M.M. Kocakerim, A quantitative comparison between electrocoagulation and chemical coagulation for boron removal from boron-containing solution, J. Hazard. Mater., 149 (2007) 475–481.
[45] U. Ayyappan, M.S. Indu, A.G. Murickan, J. Balagopal, A.S Kumar, K.L. Priya, Continuous Flow Electrocoagulation System for the Treatment of Coir Industry Wastewater, Proceedings of International Web Conference in Civil Engineering for a Sustainable Planet (ICCESP 2021), 2021, doi: 10.21467/proceedings.112.
[46] A. Srivastava, K. Srivastava, P. Singh, Application of continuous electrocoagulation process for distillery wastewater treatment, J. Sci. Ind. Res., 80 (2021) 486–490.
[47] U. Tezcan, A.S. Koparal, U.B. Ogutveren, Electrocoagulation of vegetable oil refinery wastewater using aluminum electrodes, J. Environ. Manage., 90 (2009) 428–433.
[48] H. Liu, X. Zhao, J. Qu, Electrocoagulation in Water Treatment, C. Comninellis, G. Chen, Eds., Electrochemistry for the Environ., Spring. Sci.+Bus. Med., LLC, 2010, pp. 245–262.
[49] I.A. Alaton, I. Kabdasl, D. Hanbaba, E. Kuybu, Electrocoagulation of a real reactive dye bath effluent using aluminum and stainless steel electrodes, J. Hazard. Mater., 150 (2008) 166–173.
[50] B. Merzouk, B. Gourich, A. Sekki, K. Madani, C. Vial, M. Barkaoui, Studies on the ecolorization of textile dye wastewater by continuous electrocoagulation process, J. Chem. Eng., 149 (2009) 207–214.
[51] A.R. Makwana, M.M. Ahammed, Continuous electrocoagulation process for the post-treatment of anaerobically treated municipal wastewater, Process Saf. Environ. Prot., 102 (2016) 724–733.
[52] T.L. Benazzi, M.D. Luccio, R.M. Dallago, J. Steffens, R. Mores, M.S.D. Nascimento, J. Krebs, G. Ceni, Continuous flow electrocoagulation in the treatment of wastewater from dairy industries, Water Sci. Technol., 73 (2016) 1418–1425.
[53] M. Kobya, E. Gengec, E. Demirbas, Operating parameters and costs assessments of a real dye house wastewater effluent treated by a continuous electrocoagulation process, Chem. Eng. Process. Process Intensif., 101 (2016) 87–100.
[54] O.T. Can, M. Kobya, E. Demirbas, M. Bayramoglu, Treatment of the textile wastewater by combined electrocoagulation treatment of the textile wastewater by combined electrocoagulation, Chemosphere, 62 (2006) 181–187.
[55] F. Deniz, C. Akarsu, Operating cost and treatment of boron from aqueous solutions by electrocoagulation in low concentration, Global Challenges, 2 (2018) 1800011, doi: 10.1002/gch2.201800011.
[56] Iraq Electricity Prices. Available at: www.GlobalPetrolPrices.com, https://www.globalpetrolprices.com/Iraq/electricity_prices
[57] Ingot Aluminum Iraq. Available at: https://lnfme.com/aluminium-iraq
[58] S.O. Giwa, A. Giwa, Z. Zeybek, H. Hapoglu, Electrocoagulation treatment of petroleum refinery wastewater: optimization through RSM, Int. J. Eng. Res. Technol., 2 (2013) 606–615.
[59] F. Ozyonar, B. Karagozoglu, Operating cost analysis and treatment of domestic wastewater by electrocoagulation using aluminum electrodes, Pol. J. Environ. Stud., 20 (2011) 173–179.